Recent research on EPS geofoam seismic buffers

Richard J. Bathurst and Saman Zarnani
GeoEngineering Centre at Queen's-RMC
Royal Military College of Canada
Kingston, Ontario Canada K7K 7B4
Email: bathurst-r@rmc.ca

Abstract

The paper is a synthesis of a recent body of work carried out by the writers that is focused on the use of EPS geofoam buffers for seismic load attenuation against rigid soil retaining walls. The paper begins with a description of a series of physical 1-m high reduced-scale shaking table tests that were carried out on a physical control wall and six walls constructed with EPS seismic buffers. These tests provided the first "proof of concept" by demonstrating as much as a 40% reduction in peak dynamic loads using vertical EPS buffer layers placed between the rigid wall and the granular backfill soil. Next, details of the development and verification of a displacement-based model and a FLAC numerical model are described and simulation results verified against the physical shaking table tests. The numerical results include simulations carried out with simple linear elastic constitutive models for the EPS buffers and granular soil backfill and more complex non-linear hysteretic models. The paper reports the results of a parametric numerical study that used the verified FLAC model to develop a series of preliminary design charts for the selection of a suitable seismic buffer based on characteristics of the design earthquake accelerogram. Some additional data from laboratory in-isolation dynamic (resonant column) and cyclic load testing of EPS specimens are also presented. These data are important to provide input parameters for advanced non-linear hysteretic constitutive models for EPS seismic buffers.

INTRODUCTION

The use of a vertical compressible inclusion to reduce static earth pressures against rigid earth retaining wall structures has been demonstrated in the field and in small-scale modelling by Partos and Kazaniwsky (1987), McGown and Andrawes (1987) and McGown et al. (1988). Karpurapu and Bathurst (1992) carried out a parametric study using a finite element method (FEM) numerical model that was first verified against physical test results reported by McGown and Andrawes (1987) and McGown et al. (1988). The numerical models confirmed that horizontal stresses could be reduced to "quasi-active" values and thus reduce the structural requirements of the rigid wall. The numerical models were then used to generate design charts for selection of a minimum thickness and modulus for the compressible inclusion to achieve a minimum earth pressure condition when in combination with a range of cohesionless backfill materials compacted to different densities. Today, the choice for the compressible inclusion is block-moulded low-density expanded polystyrene (EPS), or EPS "geofoam" according to modern geosynthetics terminology. A logical extension of the EPS "yielding" compressible inclusion application is the same construction technique to mitigate seismic loads. This paper summarizes the first documented "proof of concept" for EPS seismic buffers to reduce dynamic earthquake-induced earth pressures against rigid earth retaining walls using physical shaking table tests. The remainder of the paper summarizes recent research related to numerical modelling of seismic buffer tests, dynamic EPS properties, parametric numerical studies and finally a series of design charts that can be used for preliminary design of these systems.

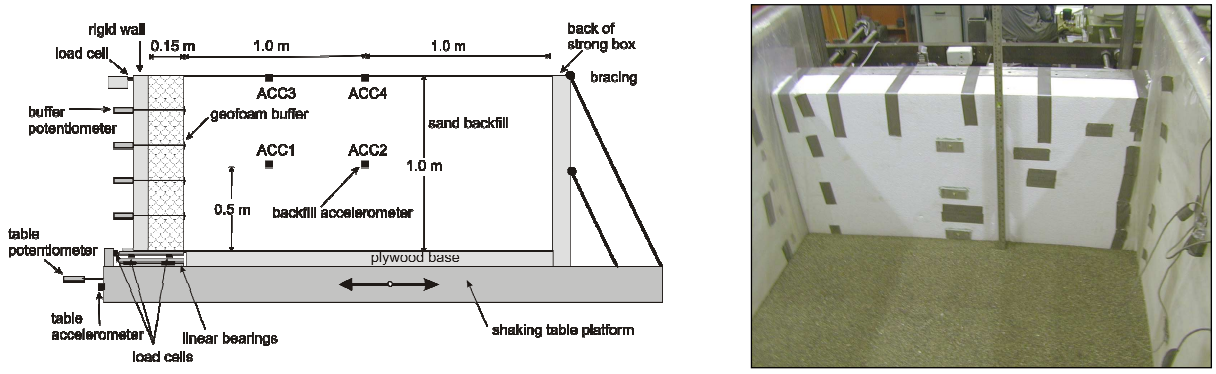

a) shaking table model with EPS geofoam buffer

b) placement of 1 m-high EPS geofoam buffer against rigid bulkhead

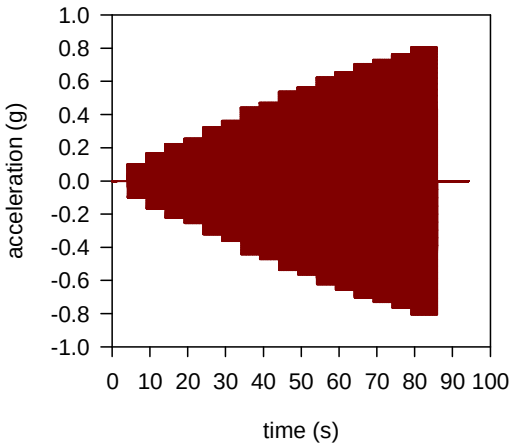

c) base excitation accelerogram

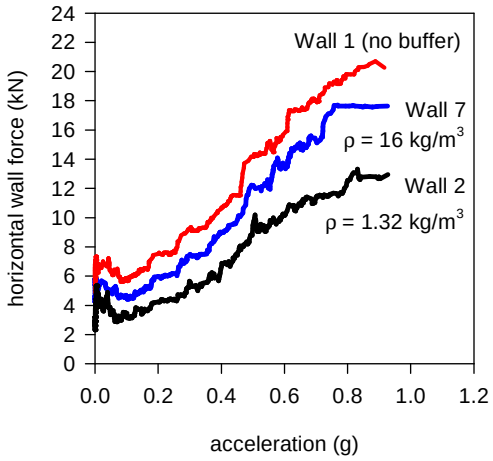

d) peak dynamic earth forces

Figure 1. Reduced-scale EPS geofoam seismic buffer shaking table tests

SHAKING TABLE TESTS

Zarnani and Bathurst (2007) and Bathurst et al. (2007a) reported the results of shaking table tests carried out on 1 m-high rigid walls with and without EPS seismic buffers, and a cohesionless soil backfill extending 2 m beyond the rigid wall (or buffer) (Figure 1a,b). The wall, seismic buffer and sand backfill were contained within a rigid strongbox fixed to the shaking table. The thickness of the geofoam was kept constant at 0.15 m. Five different EPS materials with densities ρ = 16, 14 (elasticized EPS), 12, 6 and 1.3 kg/m^3 were used. The densities below 12 kg/m^3 were achieved by removing material by drilling holes or cutting strips from the virgin EPS sheets. A stepped-amplitude sinusoidal base excitation record with predominant frequency of 5 Hz and maximum acceleration amplitude of about 0.8g was applied to the shaking table (Figure 1c). The rigid wall (bulkhead) against which the geofoam layer was placed was supported by a series of load cells which allowed the dynamic load-time history on the wall to be recorded in real time. Potentiometer-type displacement transducers were inserted through the rigid wall and attached to small plates located on the surface of the geofoam to allow permanent and dynamic compressive strain in the seismic buffer to be computed. Experimental results (Figure 1d) showed that at peak base excitation amplitude of about 0.7g the geofoam compressible inclusion reduced dynamic earth loads by 15% to 40% compared to the rigid wall case. The greatest force reduction occurred for the geofoam buffer with lowest density corresponding to the material with the lowest initial elastic tangent modulus. The reductions in dynamic loads recorded in this

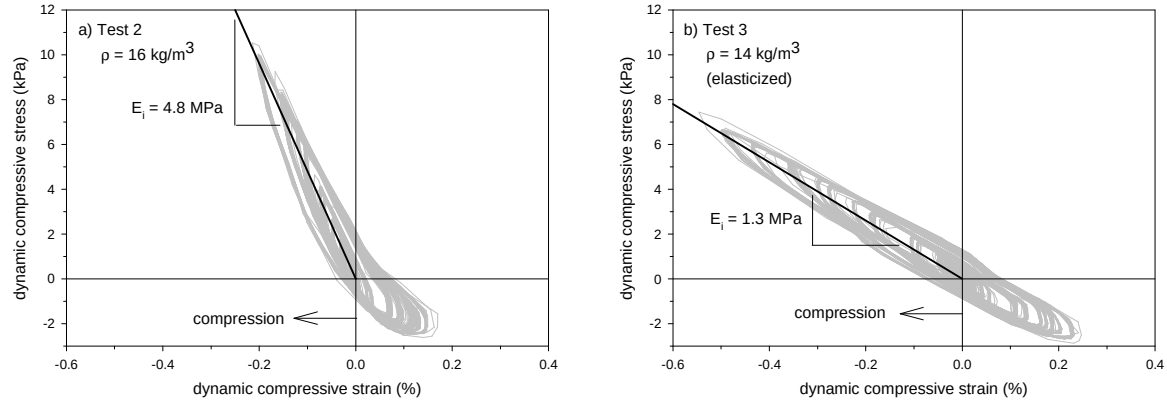

a) $\rho = 16$ kg/m^3 b) $\rho = 14$ kg/m^3 (elasticized)

Figure 2. Measured dynamic EPS buffer stress-strain loops during shaking table tests

experimental study provided "proof of concept" and the motivation for the work that is described next. A corollary benefit of the load and displacement instrumentation described earlier was that the dynamic elastic modulus of the EPS geofoam could be computed from dynamic stress-strain loops (Figure 2) and these values used in numerical models.

NUMERICAL MODELLING

Displacement Model

Bathurst et al. (2007b) proposed a simple one-block model for calculating the dynamic response analysis of seismic buffer retaining walls (Figure 3a). The soil wedge is modelled as a rigid block under plane strain conditions. The seismic buffer is located between the rigid retaining wall and soil. A linear failure plane is assumed to propagate through the backfill soil from the heel of the buffer at an angle to the horizontal that decreases with increasing magnitude of peak input acceleration. The forces at the wedge boundaries are computed using linear spring models. The compression-only force developed at the boundary between the soil wedge and geofoam buffer is computed using a single linear compression-only spring. This spring is called the buffer stiffness and is computed as K = E/b where E is the linear elastic modulus of the EPS and b is the thickness. The linear normal spring acting at the soil-soil wedge boundary permits tension and compression but was observed to develop only compressive forces during computation cycles. The shear springs at block boundaries are modelled as stress-dependent linear-slip elements to permit plastic sliding. The solution scheme is based on an explicit time-marching finite difference approach, which is commonly used for the solution of discrete element problems. The approach was modified to consider the compressible geofoam-soil boundary condition and changes in geometry of the soil wedge (block). At each time step, the numerical scheme involves the solution of the equations of motion for the block followed by calculation of the forces. The computed load-time response for an example case is presented in Figure 3b. For clarity only the peak values from the load-time record for each numerical simulation are plotted in the figure. The datum for the plot is the end of construction. Hence, these values are the result of dynamic loading only. There is generally good agreement between the physical and numerical models for the configurations up to about 70 seconds corresponding to a peak excitation acceleration of 0.7g. At higher accelerations there is likely more complex system responses that cannot be captured by the simple displacement model employed. For example, there are likely higher wall deformation modes at higher levels of base excitation. The poor predictions at peak base excitation levels likely led to the overestimation of buffer compression and loads at the end

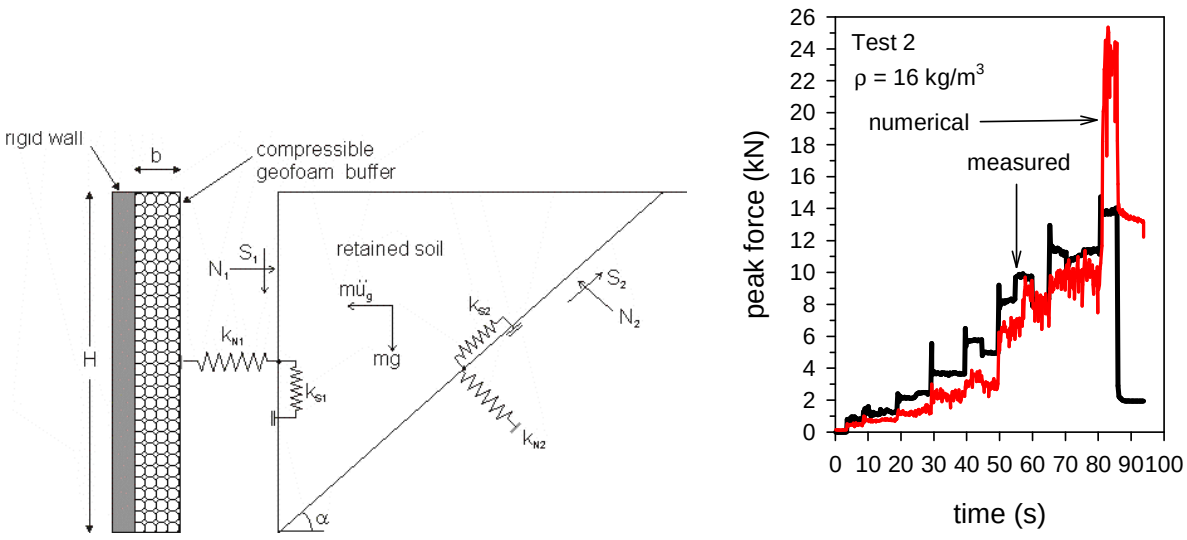

a) block model b) wall force-time history

Figure 3. Single block wall-buffer displacement model

of the tests when the walls were returned to the static condition. Nevertheless, the trends in the measured data for the two walls with respect to buffer force are generally captured by the numerical model up to about 0.7g, and in many instances there is good quantitative agreement. A peak ground acceleration value of 0.7g is a significant value in geotechnical earthquake design.

Finite Difference Method (FLAC)

Constitutive Models and Simulation of Reduced-Scale Seismic Buffer Models

Numerical simulations of the RMC reduced-scale models were also carried out using the finite difference method computer program FLAC (Itasca 2005). Two constitutive modelling approaches were used. The first model for both the sand and EPS geofoam was linear-elastic plastic with Mohr-Coulomb (M-C) criterion and Rayleigh damping (3%). The model captures hysteretic load-unload behaviour if plasticity occurs. A description of the selection of model parameters and the general modelling approach can be found in the paper by Zarnani and Bathurst (2008). The second more sophisticated model investigated by the writers is called the equivalent linear method (ELM) (Zarnani and Bathurst 2009a). This model simulates non-linear cyclic behaviour including shear modulus degradation with shear strain and strain-dependent damping ratio. The properties of the backfill sand and EPS geofoam were established from resonant column tests and cyclic uniaxial compression tests performed by the writers. Shear modulus degradation and damping ratio curves for EPS geofoam are shown in Figure 4. The data from testing performed by the writers are plotted as symbols in the figure. The 3-parameter sigmoidal function approximation to the experimental data is judged to be in reasonable agreement with the physical data from the writers and other data reported in the literature. A no-slip boundary at the bottom of the sand backfill was assumed to simulate the rough boundary in the physical tests (i.e. a layer of sand was epoxied to the bottom of the strong box container). A slip and separation interface between the buffer and the soil was specified. This interface allowed the soil and buffer to separate with no tensile stress. The base and the two vertical boundaries of the models were excited using the equivalent velocity record computed from the measured acceleration record (e.g. Figure 1c). The numerical results of interest are the peak magnitudes of horizontal force developed at end of construction and during base excitation. Maximum wall force versus time histories for two physical tests and numerical simulations with

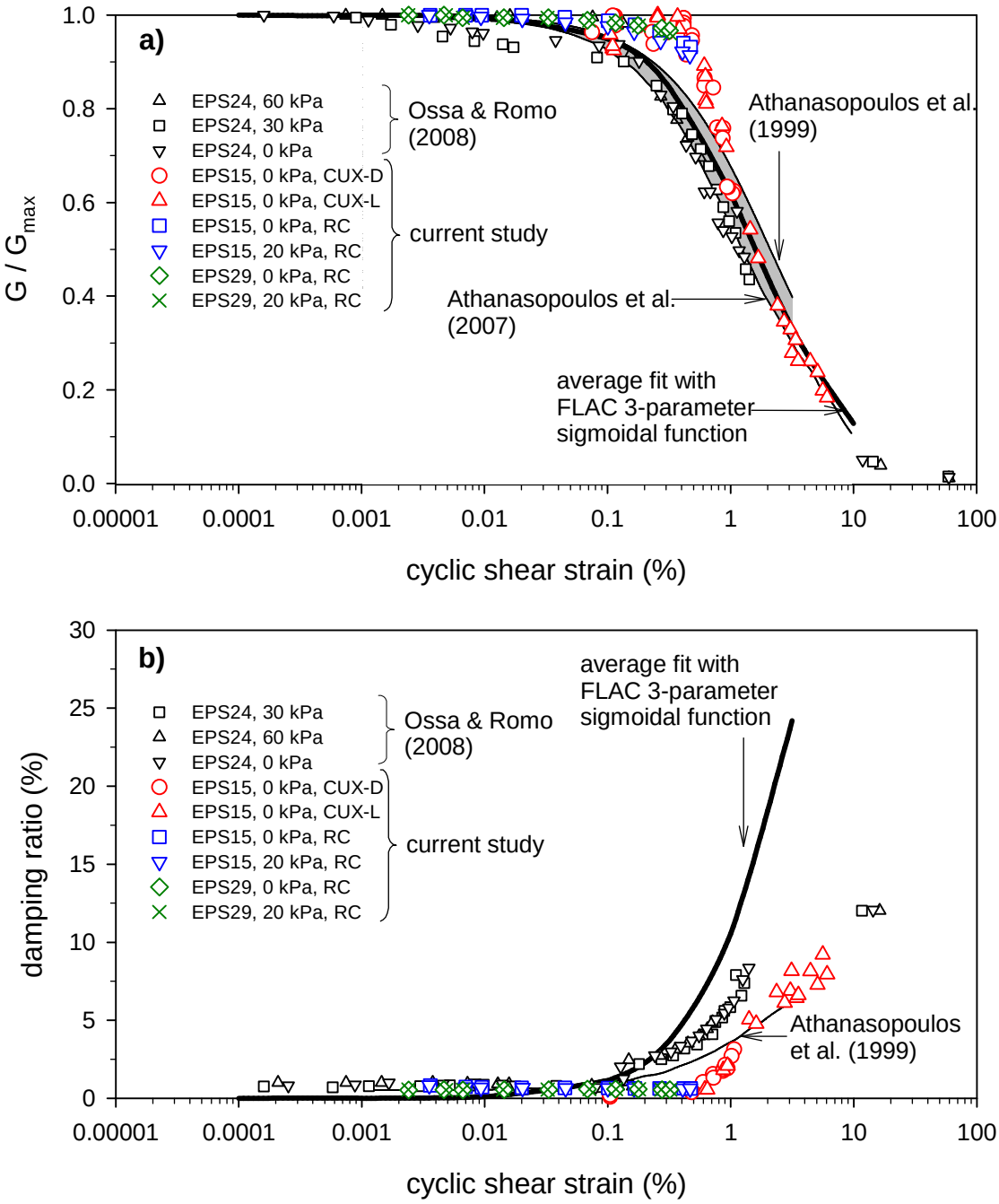

Figure 4. Variation of: a) shear modulus; b) damping ratio with cyclic shear strain amplitude for EPS geofoam

two constitutive model types are presented in Figure 5. Additional comparisons of numerical and physical tests can be found in the paper by Zarnani and Bathurst (2009a). The vertical axis in the plots corresponds to the total horizontal earth force acting against the rigid wall per unit width of wall. The figures show that there is reasonably good agreement between measured and predicted results regardless of model type. There is a noticeable discrepancy between results at the beginning of the test for Wall 4. This is believed to be due to locked-in initial horizontal stresses that may have developed as a result of the gentle initial vibro-compaction technique that was used to densify the soil during placement of the sand layers in the strong box. Both methods captured the qualitative trends in the measured load-time history of the walls and in many instances were in good quantitative agreement with measured data. In some simulations reported

by Zarnani and Bathurst (2009a) the ELM approach gave higher predictions of total peak wall forces at the final excitation level, but predictions were closer to the measured results for the seismic buffer test with the most compressible EPS material. However, if only the dynamic increment of force is considered, the simpler model was judged to be sufficiently accurate over much of the load-time history of the systems for practical purposes. Hence, the simple linear-elastic perfectly plastic model was adopted for the simulations used in the parametric analyses described in the next section.

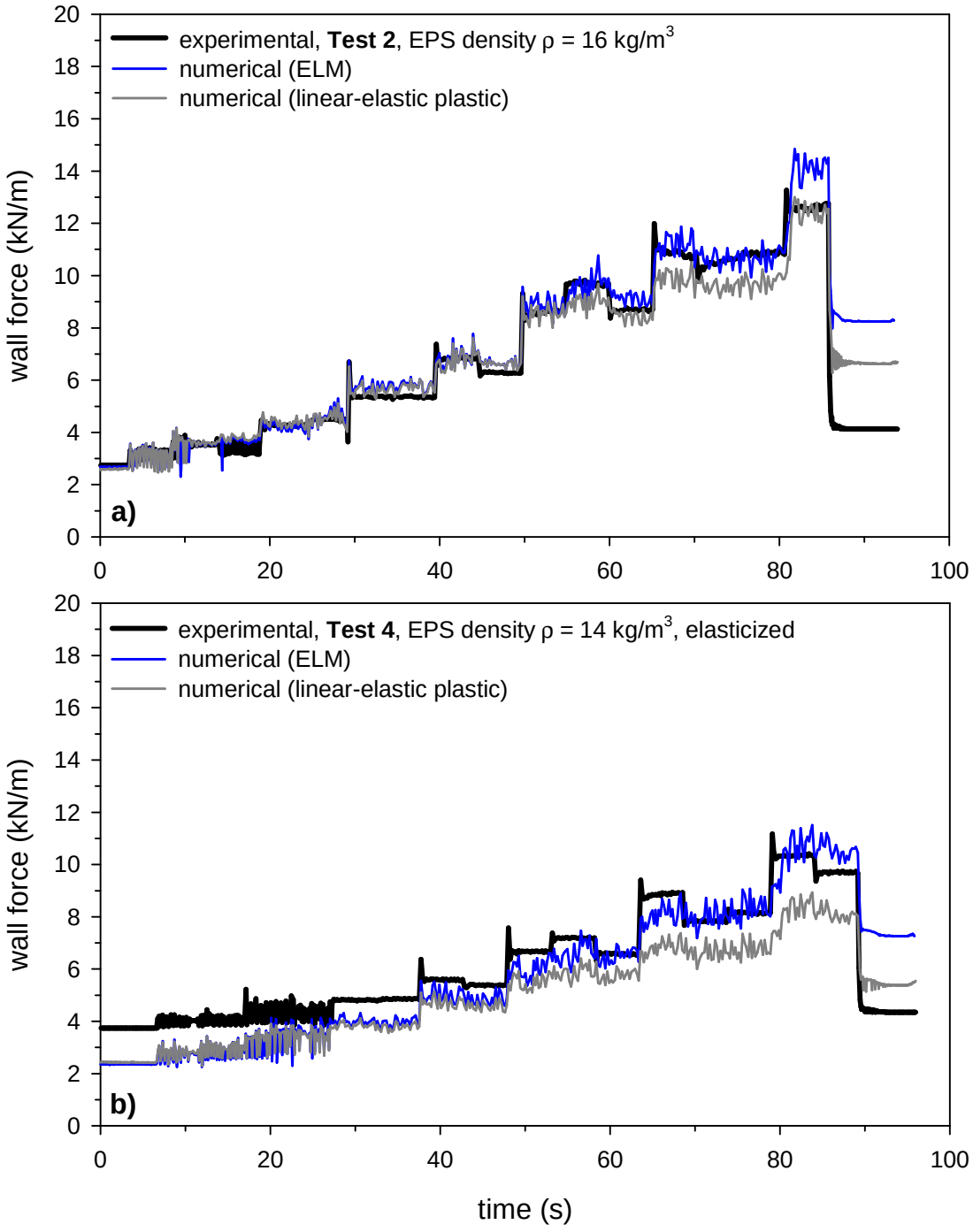

Figure 5. Total peak wall force versus time: a) ρ = 16 kg/m3; b) ρ = 14 kg/m^3 (elasticized)

Parametric Analysis

Program FLAC (Itasca 2005) was used to carry out numerical simulations of rigid walls of height H = 1, 3, 6 and 9 m with and without a geofoam seismic buffer. The walls were modelled as fully rigid with no lateral or rotational degrees of freedom. The width to height ratio of the retained soil in all simulations was constant at B/H = 5. This ratio was selected based on experience with similar numerical parametric studies on reinforced soil walls using FLAC and reported by Bathurst and Hatami (1998). They showed that the magnitudes of wall response (lateral displacements and axial reinforcement loads) are influenced by the volume of the soil behind the reinforced soil zone in numerical simulations. For example, the larger the volume, the greater the wall deformations and reinforcement loads. However, they also showed that there is diminishing effect of backfill volume on these response features for B/H > 5. Hence this ratio was fixed at five in the current study in order to minimize the numerical grid size and computation time. The thickness of the geofoam seismic buffers (b) was varied according to the ratio b/H = 0.025, 0.05, 0.1, 0.2 and 0.4. In order to minimize the possible influence of numerical grid refinement on model response, the same numerical grid density was used in all models. For example, for 1 m-, 3 m-, 6 m- and 9 m-high wall models, the mesh was generated using nodes placed on a square grid with 0.05, 0.15, 0.3 and 0.45 m centres, respectively. The mesh density was selected to match the value in the original FLAC simulations by Zarnani and Bathurst (2008) that were used to verify the numerical model in the current study. Nevertheless, a check on the sensitivity of the numerical results to mesh density was carried out by repeating simulations for a 6 m-high wall with mesh sizes of 0.3, 0.15 and 0.05 m. The difference between maximum wall forces was about 1%, which is negligible. The rigid wall was modelled with a fixed velocity boundary condition in the X direction. The far-end boundary of the retained soil had fixed velocity in both X and Y directions. The fixed X-Y velocity condition for the far-end boundary was adopted because in some simulations carried out at high excitation frequencies and only X direction fixed, the soil could flow over the top of the wall and cause numerical instability. Numerical simulations were carried out to investigate the influence of far-end boundary conditions on model results. It was found that the difference in maximum measured wall force between the two cases (far-end boundary with fixed velocity in X direction only, or fixed velocity in both X and Y directions) at low excitation frequencies was about 1%, which is negligible. Further details regarding the dynamic loading of the wall models are described in the paper by Zarnani and Bathurst (2009b). The horizontal excitation record that was applied to the bottom horizontal boundary and the two vertical boundaries of the model was a variable-amplitude sinusoidal wave with peak acceleration amplitude of 0.7g (Figure 6a) and frequencies ranging from f = 0.7 Hz to 21 Hz. The frequency values were selected to investigate the influence of proximity of input predominant frequency to the fundamental frequency of the models (ratio f / f_{11} where f_{11} is the fundamental (resonance) frequency of the system). The duration and peak acceleration amplitude of the excitation was the same in all simulations (t_{max} = 17 s and a_{max} = 0.7g, respectively). A variable-amplitude excitation record was selected because it is relatively simple to characterize compared to an actual earthquake accelerogram. Furthermore, it is not as aggressive as the same sinusoidal record applied with constant or stepped peak acceleration amplitude (Bathurst et al. 2002). The application of an actual earthquake accelerogram may appear attractive but the choice of which earthquake record to use is problematic. Nevertheless, the effect of actual scaled earthquake records and synthetic accelerograms were investigated and found not to significantly influence design chart outcomes presented later. An example of a typical wall force-time response curve for a rigid wall control case (i.e. no seismic buffer) is plotted in Figure 6b. This structure was 3 m high and was excited at a frequency that was 30% of the fundamental frequency (f_{11}) of the system. Superimposed on the figure are the peak force-time envelopes for the same wall without and with seismic buffers of varying thickness (b). The plot shows that wall forces are attenuated when a geofoam seismic

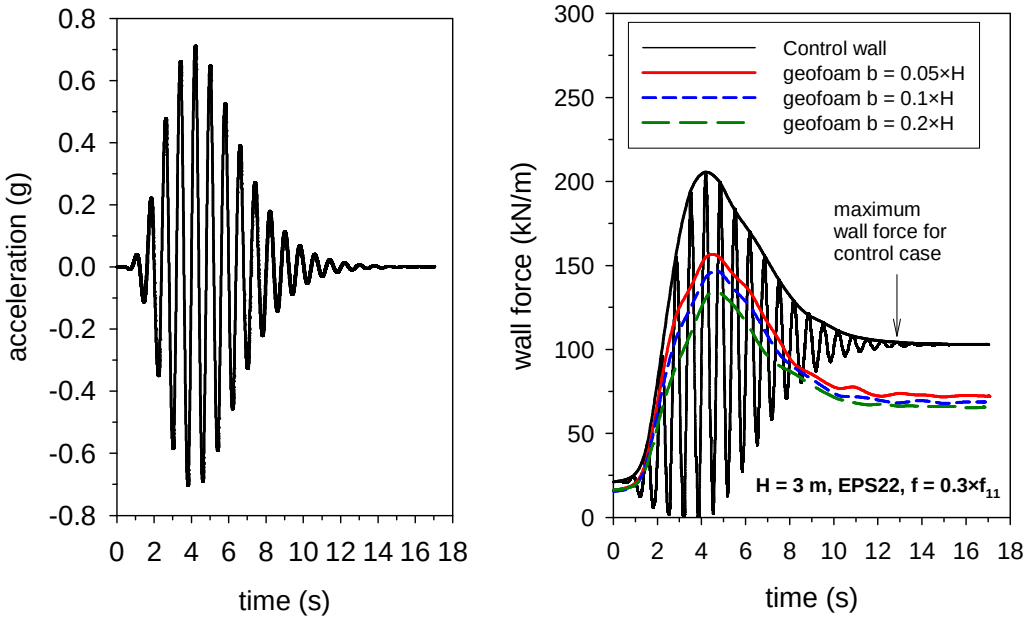

a) input excitation record b) example wall force-time response histories

Figure 6. Example wall excitation accelerogram and wall force-time responses for a 3 m-high wall with and without EPS22 (excited at 0.3 × f_{11})

buffer is placed against the back of the rigid wall compared to the control case, and the magnitudes of peak wall force decrease with increasing buffer thickness.

Preliminary Design Charts

In this numerical study, EPS19, EPS22 and EPS29 materials (according to ASTM D6817 designation system) were assumed which correspond to EPS with minimum densities of 18.4, 21.6 and 28.8 kg/m^3, respectively. The EPS geofoam was modelled as linear-elastic purely cohesive material and the soil as a linear-elastic perfectly plastic material with M-C failure criterion and Rayleigh damping. Numerical investigations described earlier showed that this was satisfactory based on comparison with physical test results and results of simulations using the more sophisticated ELM approach. Independent laboratory testing has shown that non-elasticized EPS geofoam typically behaves linear elastic up to about 1% strain. There are correlations available in the literature that relate the density of geofoam to initial tangent Young's modulus, Poisson's ratio, compressive strength and tensile strength (e.g. Zarnani and Bathurst 2007). Initial stiffness values of non-elasticized geofoam materials reported in the literature were similar to the measured dynamic stiffness of the EPS seismic buffer in the shaking table test program (e.g. Figure 2a). Hence, the initial stiffness from conventional compression tests can be used for parameter E to compute buffer K = E/b for non-elasticized EPS. However, for elasticised geofoam, the back-calculated elastic modulus values from the shaking table tests (e.g. Figure 2b) were higher than the value reported by the manufacturer. Regardless, it is up to the designer to select project-specific values for use in the design charts or in numerical simulations of the type described in this paper. The results of simulations in this numerical parametric study are presented in the form of design charts in Figure 7. In these charts the practical quantity of interest to attenuate dynamic loads is the buffer stiffness introduced earlier and defined as the ratio of EPS elastic Young's modulus to EPS thickness. This is the same parameter used in the displacement model to quantify the stiffness of the geofoam layer (Figure 3a). Combinations of materials with different modulus and thickness can provide the

same dynamic load reduction. Hence numerical parametric results are presented in Figure 7 with K as the independent parameter and isolation efficiency as a quantitative measure of the improvement in seismic load reduction. Isolation efficiency of the seismic buffer is defined as the ratio of change in wall force between rigid and seismic buffer cases divided by peak wall force without the buffer. For each wall height, isolation efficiency versus stiffness curves fall into narrow bands based on frequency ratio and these curves are sensibly independent of buffer density. The difference in curves based on predominant frequency values of $0.3f_{11}$ and $1.4f_{11}$ diminishes with increasing wall height. In all cases there is a highly non-linear reduction of isolation efficiency with increasing buffer stiffness. Taken together, the data plots suggest that K $\leq$ 50 MN/m^3 is the practical range for the design of these systems. More results and discussion related to this parametric study are reported by Zarnani and Bathurst (2009b).

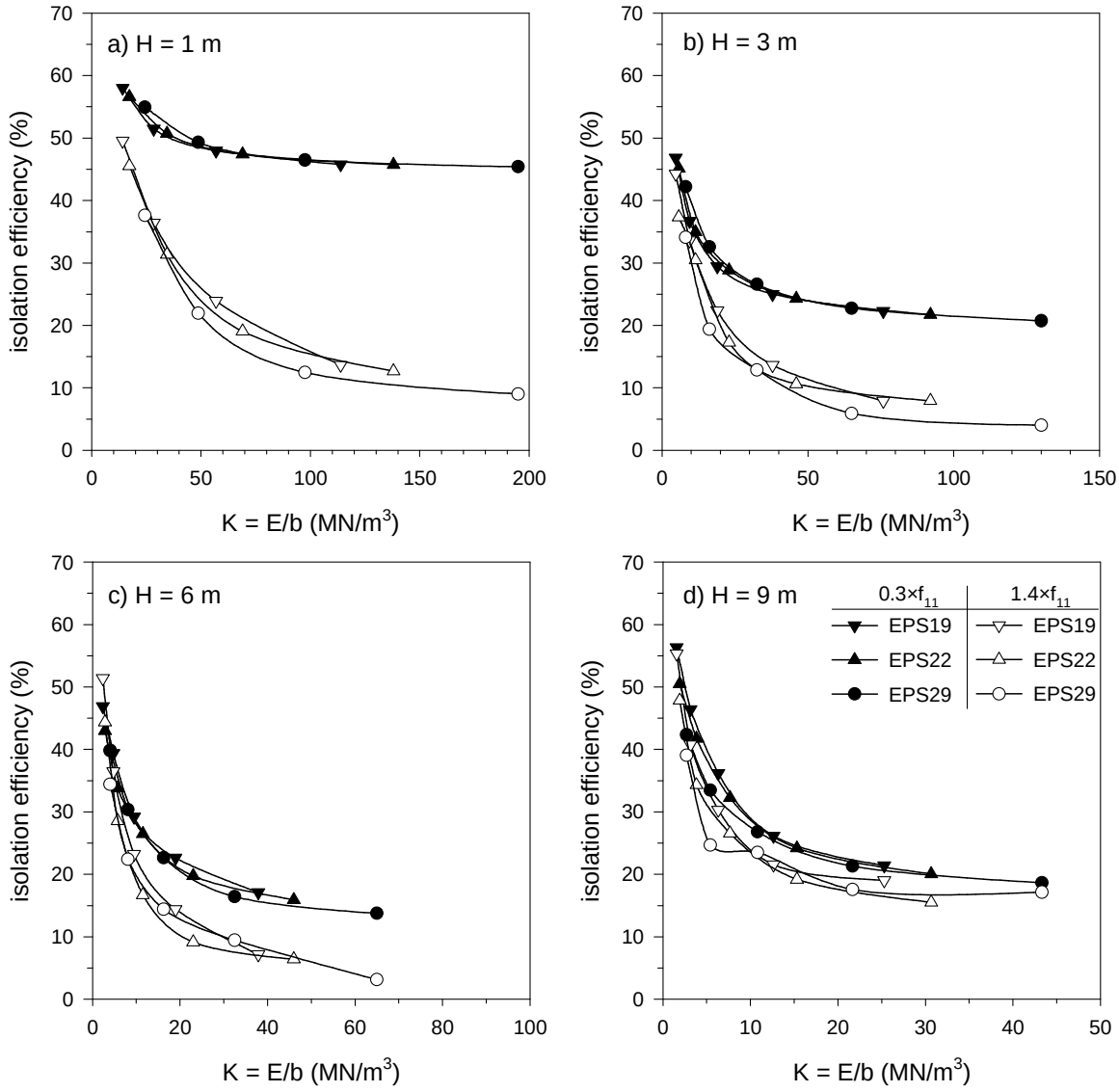

Figure 7. Preliminary EPS seismic design charts for different wall heights

CONCLUSIONS

This paper provides a synthesis of recently published work by the writers on both experimental and numerical simulation work related to EPS seismic buffers to reduce earthquake-induced loads against rigid retaining wall structures. Validated FLAC numerical models were used to carry out a parametric analysis to investigate the influence of wall height, EPS geofoam type,

thickness, stiffness and excitation record on seismic buffer performance. The major practical outcome of this research is the identification of buffer stiffness (defined as K = E/b where E is the elastic modulus and b is thickness) as the parameter of interest to design these systems. For the range of parameters investigated, $K \leq 50$ MN/m^3 was observed to be the practical range for the design of these systems to attenuate earthquake loads against rigid retaining wall systems.

REFERENCES

1. ASTM D 6817-06 2006. Standard Specification for Rigid Cellular Polystyrene Geofoam. American Society for Testing and Materials, West Conshohocken, PA, USA.
2. Athanasopoulos, G.A., Nikolopoulou, C.P., Xenaki, V.C. and Stathopoulou, V.D. 2007. Reducing the seismic earth pressure on retaining walls by EPS geofoam buffers–numerical parametric study. 2007 Geosynthetics Conference, Washington, DC., USA, 15 p.
3. Athanasopoulos, G.A., Pelekis, P.C. and Xenaki, V.C. 1999. Dynamic properties of EPS geofoam: An experimental investigation. Geosynthetics International, 6(3): 171-194.
4. Bathurst, R.J. and Hatami, K. 1998. Seismic response analysis of a geosynthetic reinforced soil retaining wall. Geosynthetics International, 5(1-2): 127-166.
5. Bathurst, R.J., Hatami, K. and Alfaro, M.C. 2002. Geosynthetic reinforced soil walls and slopes: Seismic aspects. Geosynthetics and Their Applications (S.K. Shukla Ed.), Thomas Telford, 327-392.
6. Bathurst, R.J., Zarnani, S. and Gaskin, A. 2007a. Shaking table testing of geofoam seismic buffers. Soil Dynamics and Earthquake Engineering, 27(4): 324-332.
7. Bathurst, R.J., Keshavarz, A., Zarnani, S. and Take, A. 2007b. A simple displacement model for response analysis of EPS geofoam seismic buffers. Soil Dynamics and Earthquake Engineering, 27(4): 344-353.
8. Itasca Consulting Group. 2005. FLAC: Fast Lagrangian Analysis of Continua, version 5.0. Itasca Consulting Group, Inc., Minneapolis, Minnesota, USA.
9. Karpurapu, R. and Bathurst, R.J. 1992. Numerical investigation of controlled yielding of soil-retaining wall structures. Geotextiles and Geomembranes, 11(2): 115-131.
10. McGown, A. and Andrawes, K.J. 1987. Influence of wall yielding on lateral stresses in unreinforced and reinforced fills. Research Report 113, TRRL, Crowthrone, Berkshire, UK.
11. McGown, A., Andrawes, K.Z. and Murray, R.T. 1988. Controlled yielding of the lateral boundaries of soil retaining structures. ASCE Symposium on Geosynthetics for Soil Improvement, ed. R. D. Holtz, Nashville, TN, USA, 9 May 1988, 193-211.
12. Ossa, A. and Romo, M.P. 2008. A model for EPS dynamic shear modulus and damping ratio. First Pan American Geosynthetics Conference and Exhibition, 2-5 March 2008, Cancun, Mexico, pp. 894-901.
13. Partos, A.M. and Kazaniwsky, P.M. 1987. Geoboard reduces lateral earth pressures. In Proceedings of the Geosynthetics'87, IFAI, New Orleans, LA, USA, 24-25 Feb 1987, 628-639.
14. Zarnani, S. and Bathurst, R.J. 2007. Experimental investigation of EPS geofoam seismic buffers using shaking table tests. Geosynthetics International, 14(3): 165-177.
15. Zarnani, S. and Bathurst, R.J. 2008. Numerical modeling of EPS seismic buffer shaking table tests. Geotextiles and Geomembranes, 26(5): 371-383.
16. Zarnani, S. and Bathurst, R.J. 2009a. Influence of constitutive model on numerical simulation of EPS seismic buffer shaking table tests. Geotextiles and Geomembranes, 27(4): 308-312.
17. Zarnani, S. and Bathurst, R.J. 2009b. Numerical parametric study of EPS geofoam seismic buffers. Canadian Geotechnical Journal, 46(3): 318-338.